Metallophysics and Advanced Technologies
Металофіз. новітні технол.
Metallofiz. Noveishie Tekhnol.
2019, vol. 41, No. 3, pp. 375–388
https://doi.org/10.15407/mfint.41.03.0375
Reprints available directly from the publisher

© 2019 G. V. Kurdyumov Institute for Metal Physics,
National Academy of Sciences of Ukraine
Published by license under
the G. V. Kurdyumov Institute for Metal Physics–
N.A.S. of Ukraine Publishers imprint.
Printed in Ukraine.

INTERACTIONS OF RADIATION AND PARTICLES WITH CONDENSED MATTER

PACS numbers: 07.85.Jy, 07.85.Qe, 61.05.cc, 87.57.cj, 87.59.-e

Solving of Direct and Inverse Scattering Problems for Heterogeneous Non-Crystalline Objects in Analyzer-Based Imaging

G. O. Velikhovskyi, V. B. Molodkin, V. V. Lizunov, T. P. Vladimirova, S. V. Lizunova, Ya. V. Vasylyk, M. P. Kulish[*], O. P. Dmytrenko[*], and O. L. Pavlenko[*], Iu. V. Davydova[**]

G. V. Kurdyumov Institute for Metal Physics, N.A.S. of Ukraine,
36 Academician Vernadsky Blvd.,
UA-03142 Kyiv, Ukraine
[*]*Taras Shevchenko National University of Kyiv,*
60 Volodymyrska Str.,
UA-01033 Kyiv, Ukraine
[**]*State Institution 'Institute of Pediatrics, Obstetrics and Gynecology Named after Academician O. M. Lukyanova, NAMS of Ukraine',*
8 Platona Mayborody Str.,
UA-04050 Kyiv, Ukraine

This article introduces a theoretical model for analyzer-based imaging of non-crystalline objects that takes into account the impact of microscopic and macroscopic heterogeneities within the object as well as the instrumental factors. The model includes particular phase variational features required for solving the inverse scattering problem. It provides the possibility to reconstruct the shape of the object from a set of intensity profiles.

Key words: X-ray optic, phase-contrast imaging, dynamical diffraction theory.

В роботі розвинуто теоретичну модель, яка у тривісьовій схемі формуван-

Corresponding author: Vyacheslav Vyacheslavovych Lizunov
E-mail: lizunov.vyacheslav@gmail.com

Citation: G. O. Velikhovskyi, V. B. Molodkin, V. V. Lizunov, T. P. Vladimirova, S. V. Lizunova, Ya. V. Vasylyk, M. P. Kulish, O. P. Dmytrenko, O. L. Pavlenko, and Iu. V. Davydova, Solving of Direct and Inverse Scattering Problems for Heterogeneous Non-Crystalline Objects in Analyzer-Based Imaging, *Metallofiz. Noveishie Tekhnol.*, **41**, No. 3: 375–388 (2019), DOI: 10.15407/mfint.41.03.0375.

ня топографічних зображень некристалічних об'єктів враховує вплив мікро- та макронеоднорідностей в об'єкті, а також інструментальних факторів. При цьому в моделі встановлено і враховано необхідні для розв'язку оберненої задачі фазоваріаційні особливості, чим забезпечено можливість відтворення форми об'єкту з набору профілів інтенсивності.

Ключові слова: рентгенівська оптика, фазоконтрастні зображення, динамічна теорія дифракції.

В работе развита теоретическая модель, которая для трёхосевой схемы формирования топографических изображений некристаллических объектов учитывает влияние микро- и макронеоднородностей в объекте, а также инструментальных факторов. При этом в модели установлены и учтены необходимые для решения обратной задачи фазовариационные особенности, чем обеспечена возможность восстановления формы объекта по набору профилей интенсивности.

Ключевые слова: рентгеновская оптика, фазоконтрастные изображения, динамическая теория дифракции.

(Received October 22, 2018)

1. INTRODUCTION

One of the most promising ways to improve the quality of topographic images is the development of phase-contrast imaging. Amongst different methods the analyzer-based imaging (ABI) is one of the best for studying weakly-absorbing objects due to its extreme angular sensitivity for scattered radiation and low background [1–3]. This method allows to achieve high-resolution images for the objects of microscopic size with relatively simple optical scheme and is already widely used for the analysis of bio-medical samples, nuclear energy materials and lots of other cases.

The implementation of the method requires the usage of monochromator and analyzer crystals placed on the high resolution goniometer. The monochromator forms the scanning beam with defined distribution of intensity that is homogeneous within the plane perpendicular to the propagation direction. As a result of interaction with the sample the beam refracts at the small angles and its parameters (such as the wave vector, wave amplitude, angular distribution of intensity) become locally changed. These changes depend on the local characteristics of object's heterogeneity; those are being described by introducing the concepts of columns and layers for macroscopic heterogeneities, and fluctuations of composition for microscopic heterogeneities.

During the last years, a lot of works dedicated to the ABI were published (see, for example, [4–14]). However the theoretical background in most of these works was based on a number of approxima-

tions, those simplify the calculations, but restrict from taking into account the influence of a large number of parameters on the image. The present article introduces the analysis of the approximations used in simplified calculation schemes and takes into account the impact of additional parameters of the sample object and optical scheme elements with the purpose of improving the sensitivity and informativeness of the phase-contrast diagnostics and decreasing the instrumental errors.

2. THE INFLUENCE OF OBJECT'S INHOMOGENEITY AND INSTRUMENTAL FACTORS ON THE INTENSITY DISTRIBUTION

All further calculations are made using the model, suggested in [15–17]. The model allows taking into account the effects of dynamical scattering in both the monochromator and the analyzer, as well as in the non-crystalline object. This provides a possibility to establish analytical connection between the characteristics of the object and the parameters of its X-ray image. The key feature of the model is the column approximation. According to that, the space is virtually divided into narrow columns, parallel to the scanning beam. The size of the column should not exceed the diffraction limit and it should be small enough to allow considering the surface of the object within a single column as flat. In that case, the exact shape of the object would be approximately described by the orientation of such surfaces in each column. In addition, the minimal size of the column is limited with the assumption of non-overlapping columns. It means that because of sufficiently narrow angular distribution of the scanning beam intensity and small refraction angles the intensity would not redistribute between different columns. It will be shown later that in some cases the possible effect of redistribution could be easily taken into account.

Another limit for the minimal size of the column is the condition of homogeneity the object within each column and each layer. The potential of interaction of radiation and matter was considered macroscopically homogeneous, which allowed to use the refractive index.

The usage of current model provides the possibility to resolve the inverse scattering problem and reconstruct the parameters of the sample object.

2.1. The Influence of Monochromator and Analyzer Reflection Curves on the Intensity Distribution

In order to form quasi-monochromatic wave front with the small divergence angle (of the order of angular seconds) the monochromator crystal is being used. Commonly it is nearly single crystal with a very

narrow reflection curve, which in particular allows achieving the beam with required narrow intensity distribution. After scattering on the non-crystalline object, the beam propagates to analyzer, which one more nearly ideal single crystal with the respectively narrow reflection curve and then the detector measures final intensity of the beam.

The measured intensity equals to the convolution of the intensity angular distribution of the beam before the analyzer and the reflection curve of the analyzer, considering the refraction angle and possible orientational displacement of the analyzer relatively to monochromator. In that case, when the object may be considered as homogeneous (*i.e.* neglect micro-heterogeneities) the intensity distribution after the transition through the column remains of the same shape but shifted by the refraction angle and with the lowered amplitude due to absorption.

It is often convenient to find the dependency of resulting intensity from the angle of analyzer's displacement without the object at all. The usage of such curves (which will be further called convolution curves) allows in a number of cases to significantly simplify the calculations for homogeneous objects. First of all it allows to separately study the propagation of radiation within the sample object and the monochromator and analyzer crystals. Meanwhile in order to describe the propagation of the beam within the non-crystalline object the common approach is to use the approximation of geometric optics and the Snell's law. Secondly, the convolution curve contains all the information required to find the refraction angle. For that reasons the calculation or directly measuring of this curve it is possible to accelerate the processing of the experimental data. In addition, selecting single crystals with various reflection curves it is possible to purposeful achieve the convolution curve of the exact shape, required for the analysis of the object of the particular shape and composition.

However, if the object has significant inhomogeneities those distort the intensity distribution of the beam, scattered by the object, the application of described approach could cause significant errors. In that case, it is necessary to describe sequentially the interaction of the beam and the monochromator, the object (all of its layers) and the analyzer for each column. In particular, for multilayer objects it is convenient to replace the angular intensity distribution with a set of 'microbeams', each for a different angle of the beam propagation. In this way, the calculation of the convolution integrals for each layer becomes replaced with the calculation of redistribution of intensities between individual 'microbeams' and the single convolution with the reflection curve of the analyzer crystal. This greatly simplifies the calculations by decreasing the complexity from $O(N^M)$ to $O(MN^2)$, where N — the number of integration steps for each layer, M — the number of layers.

Figure 1 shows the convolution curves for the radiation Mo$K_{\alpha 1}$ ($\lambda = 0.07$ nm) for two perfect single crystals Si; the crystal No. 1 has thickness 5.4 mm, reflex (111), the crystal No. 2 has thickness 21.6 mm, reflex (333). Hereinafter, the intensity is given in relative units, proportional to the magnitude of the radiation reflected by the analyzer crystal.

The calculations show that selection of the proper monochromator and analyzer crystals allows forming the convolution curve with in advance determined parameters. In particular, the usage of the monochromator and the analyzer in the Bragg diffraction geometry allows achieving the convolution curve with sharp peak, relatively small angle at half maximum and smooth attenuation.

At the same time the usage of the monochromator in the Bragg diffraction geometry and the analyzer in the Laue diffraction geometry gives a more smooth peak but larger angle at half maximum and more rapid attenuation. Thus properly selecting the thickness of the crystals and the diffraction geometry it is possible to control the angle at half maximum and the amplitude of the convolution curve. For instance, weakly refracting materials require the usage of convolution curves with larger angle at half maximum, those provide better contrast, but the materials with greater refraction index require using wider convolution curves, those provide better signal to noise ratio further from the peak.

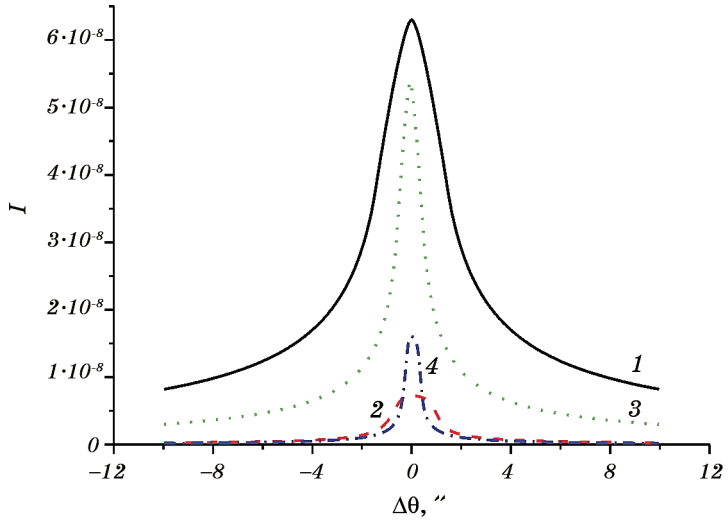

Fig. 1. The convolution curves for different pairs of crystals: the monochromator crystal No. 1 (*1*, *2*) and No. 2 (*3*, *4*) in the Bragg diffraction geometry, the analyzer crystal No. 1 (*1*, *2*) and No. 2 (*3*, *4*) in the Bragg diffraction geometry (*1*, *3*) and Laue diffraction geometry (*2*, *4*).

2.2. The Influence of Surface Inhomogeneities on the Intensity Distribution

In the case, when the object's surface has curved or rough shape, in addition to the approximation by flat surface that gives refraction angle, it is necessary to take into account the changes of angular intensity distribution, caused by these inhomogeneities. The simple heuristic way to do that is to assume that after passing through such surface each microbeam would be re-scattered with some new intensity distribution. The profile, used to apply such re-scattering could be calculated or measured in advance for every required material.

The plots on Figure 2 demonstrate the influence of the changes of intensity distribution within the scanning beam, caused by the surface inhomogeneities, on the final measured intensity. The calculation is made for a half-cylinder made of borosilicate glass of 0.31 mm radius with the round bulge. The radius of the bulge is 0.1 mm. In order to take into account the scattering caused by inhomogeneities, it was assumed that the incident plane wave would be blurred by Gaussian distribution.

The results of calculations shows that if the blur is present (*i.e.* intensity distribution changes) the peaks become greatly smoothed and the intensity after analyzer crystal decreases. Considering this effect is essential for correct calculations of non-crystalline object's parameters.

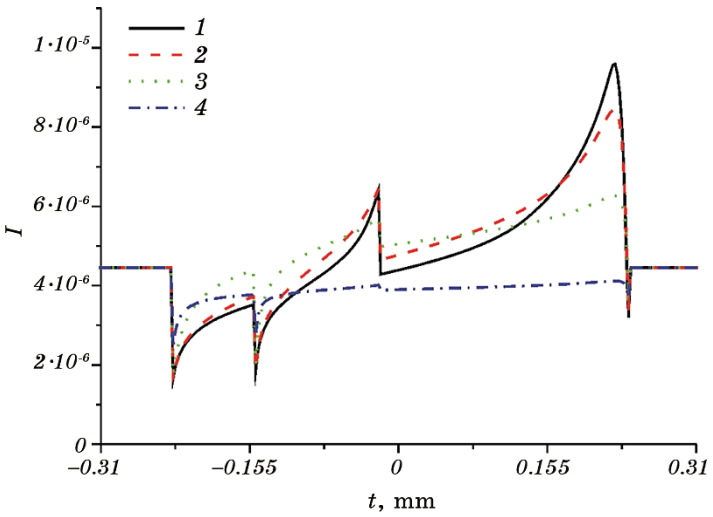

Fig. 2. The intensity profiles for the different blurring: no blurring (*1*), Gaussian blurring with half-width equal to 0.75″ (*2*), 2″ (*3*) and 5″ (*4*).

2.3. The Influence of the Fluctuation of Composition on the Intensity Distribution

When passing through the object the microbeams in addition to refraction may be absorbed and scattered on the inhomogeneities of each layer of the matter. Both effects depend on the thickness of the layer. The absorption is being taken into account as the exponential decrease of the intensity of microbeams sequentially in each layer with the use of respective absorption factors. At the same time the changes of intensity distribution caused by inhomogeneities (*i.e.* diffuse scattering) should also be calculated.

Let us consider the case, when characteristic dimensions of microscopic inhomogeneities are much smaller than the dimensions of columns and/or layer, whereas the number of these inhomogeneities is large enough. In order to find their impact let us virtually split the column into small homogeneous unit volumes, such that the distribution of inhomogeneities would be uniform within each unit volume. The diffuse scattering for microdefects of different types in crystals were studied by M. O. Krivoglaz [18]. However in the current case, when the sizes and the type of microscopic inhomogeneities may vary, the resulting change in the wave vector (after exiting the column) will be random variable. According to that, considering the central limit theorem the resulting profile will be Gaussian curve.

In particular, for two Gaussians we have:

$$\int g(u - x_0, w_1) g(x - u, w_2) du = g(x - x_0, w_1 + w_2),$$

where w_1, w_2 are respectively the squares of dispersions. Thus for the convolution of two Gaussians the resulting curve is also a Gaussian with the square of dispersion equal to the sum of dispersion squares of original curves.

The result of interaction of the beam and the whole column will be described by N convolutions, those represent the sequential scattering on the N unit volumes. Since, with all the approximations, it can be assumed that the refraction curve of a single unit volume is a Gaussian, we have:

$$\lim_{N\to\infty} \int \ldots \int du_1 \ldots du_N g_1(u_1 - x_0, w_1) g_2(u_2 - u_1, w_2) \ldots g_N(u_N - x, w_N) = \\ = g(x_0 - x, W),$$

where g_i is refraction curve of a single unit volume,

$$W = \lim_{N\to\infty} \sum_{i=1}^{N} w_i \to \int dw$$

is total blurring for the column. Similar analysis of Gaussian approxi-

mation for the scattering on the microstructures was used, for example, in article [19].

In this way, in the case of scattering on the large number of microscopic inhomogeneities resulting diffraction curve may be calculated as the Gaussian with the respective width. The blurring could be calculated from the material parameters and the thickness of the layer. For uniformly distributed inhomogeneities the blurring would be equal to $W = \kappa l$, where κ is the widening per unit length.

Finally, the angular intensity distribution of the beam equals to the convolution of the incident beam intensity and the refraction curve of the column.

In addition, when the distribution of the impurities is random and the contribution of mean-square fluctuations is small, the changes of the orientation angles of the diffuse-scattered beams may be significantly greater than the refraction angles. In such cases the column approach is unsuitable because it becomes necessary to take into account the scattering of the beams between different columns. Moreover for each column and each layer diffuse waves of different wave vectors would scatter between each other and the incident wave. All these effects were named the extinction effects caused by diffuse scattering and thoroughly studied in [20].

In present article, the effects of diffuse scattering are limited to a consideration of only the scattering on the fluctuations of atomic amplitudes and may be taken into account according to [20]. In most of the cases, their contributions are small and similar for each layer of each column and have almost no effect on the images of non-crystalline objects.

Experimentally indirect measurement of the final intensity profile may be performed by measuring the dependence of full intensity after the analyzer from the displacement angle of analyzer relatively to monochromator $I(x)$ and solving the equation:

$$I(x) = \int f(y)R(x - y)dy,$$

where f is intensity profile being searched for, R is analyzer refraction curve.

If R goes to delta-function, the calculation of intensity profile becomes trivial. This can be reached by selecting such monochromator and analyzer crystals that the analyzer refraction curve was much more narrow that the monochromator refraction curve.

2.4. The Influence of Scale Factors on the Intensity Distribution

The implementation of ABI, as well as a number of other phase-contrast methods, requires some distance between the sample and the

analyzer crystal. This distance may be large enough so that despite the small refraction angles some part of the microbeams intensity will transfer to nearby columns.

Figure 3 shows the intensity profiles for the borosilicate glass half-cylinder of 0.31 mm radius calculated with different distance from the half-cylinder to the analyzer.

One may notice that if the distance is large enough the redistribution of intensity between columns cannot be neglected. The impact of distance changes was experimentally studied in [21]. The results of that work were used to develop the 'hybrid' imaging method. It was shown that the measured profiles are significantly different from the conventional ABI profiles where the distance between the object and the analyzer is small. Thus by changing the position of analyzer crystal (both spatial and angular) it is possible to purposefully change the shape of the intensity profile and as a result improve the quality of the image.

Figure 4 demonstrate the difference between the intensities calculated with the use of the convolution curve and those calculated by sequentially applying the influence of scattering on each layer of material. The calculations performed for borosilicate glass half-cylinder.

For the homogeneous material and zero distance from the object to the analyzer, the intensity curves calculated with the use of the convolution curve and those calculated with the sequentially applying of scattering for each layer (full method) perfectly match. However, if the microscopic inhomogeneities are present and the distance from the

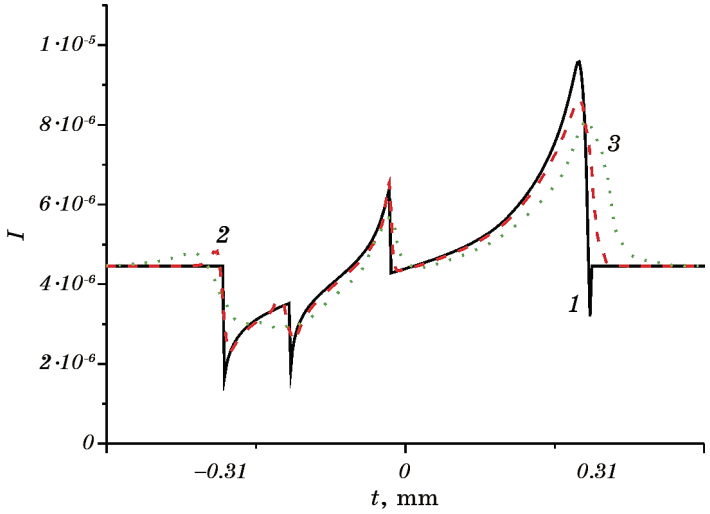

Fig. 3. The intensity profiles for the different distances from the object to the analyzer: 0 m (*1*), 1 m (*2*) and 5 m (*3*).

object to the analyzer is not zero (which causes redistribution of intensity between columns), the curves, calculated with these two methods, are significantly different. The curve, calculated using the full method, has smoothen peaks and pits, and also has the 'highlights' as the intensity slightly higher than the background near the edge of the object. The curve, calculated using the convolution curve has the peaks and pits similar to the homogeneous case but has different amplitude, and the 'highlights' near the edges of the object are absent. The nature of the amplitude changes is also different for two methods.

For all that reasons, in the case of heterogeneous non-crystalline objects it is essential to calculate the scattering step-by-step for each layer in order to avoid significant errors.

3. THE INVERSE SCATTERING PROBLEM

The main objective of all diagnostics methods is finding the parameters of the sample from experimentally measured data. This section describes general scheme and the example of shape reconstruction of simple model object by processing theoretically calculated (model) intensity profiles.

For simplicity, the half-cylinder with small round bulge on the top was chosen as the object. After virtual splitting each column will have two unknown parameters, those are the thickness and the tilt angle of entry surface. The presence of the bulge allows showing the influence

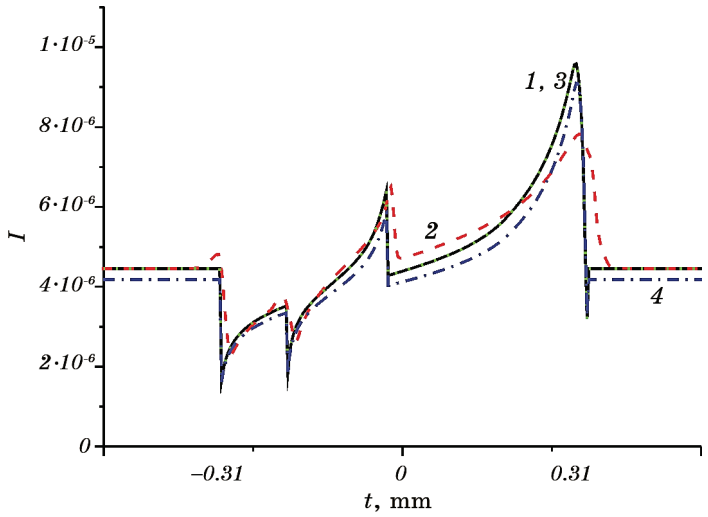

Fig. 4. The intensity profiles with zero distance and no blurring (*1*, *3*) and distance equal to 1 m with 0.75″ Gaussian blurring (*2*, *4*). Calculated using the full method (*1*, *2*) and the convolution curve (*3*, *4*).

of the surface inhomogeneities of various scales. For simplicity, the material of the object was considered homogeneous.

3.1. Calculation of Geometric Parameters of the Object

The important feature of the suggested model is the possibility to analytically determine the refraction angle. In order to do that first one need to measure or calculate the convolution curve. Afterwards the intensity profile is captured for different analyzer displacement angles and then from the system of equations the refraction angle can be found:

$$I_1 = Af_1(\varphi),$$
$$I_2 = Af_2(\varphi),$$

where $f_1(\varphi) = f(\varphi + \Delta\varphi_1)$ and $f_2(\varphi) = f(\varphi + \Delta\varphi_2)$ respectively, and f is the convolution curve.

By dividing the first equation by the second equation (and thus excluding the absorption), we have the equation for the refraction angle

$$I_2 f_1(\varphi) = I_1 f_2(\varphi).$$

It should be noted that the solution of the equation for the refraction angle depends on the shape of the convolution curve and the angular displacements. For that reason, it is necessary to find in advance the maximal refraction angles possible for the object and use such monochromator and analyzer crystals that the equation for the refraction angle had a unique solution.

Then, having the refraction angle and knowing the refractive index of the material n, one may find the tilt angles α of entrance surface of the object:

$$\varphi = \Delta n \tan(\alpha),$$

where Δn is the change of refractive index when the beam passes from one layer to another.

For the multilayer objects, the calculation of the shape of the surface is much more complicated, as the resulting refraction angle is the linear combination of contributions of each layer/surface:

$$\varphi = \sum \Delta n_i \tan(\alpha_i).$$

This case is thoroughly studied in work [16].

Another parameter of the object is the thickness of each column.

Having the refraction angle, or in the case when refraction angle does not contribute to the intensity (for example in scheme without the analyzer) it is possible to calculate the decrease of the beam intensity as a result of absorption after passing through the object and thus find its thickness from the equations:

$$A = I_1/f_1(\varphi) = I_2/f_2(\varphi) = e^{-\mu L},$$
$$L = -\ln(A)/\mu.$$

Having the thickness and the surface tilt angle for each column it is possible to reconstruct the shape of the object.

3.2. Reconstructing the Shape of the Object

For each particular material, depending on its nature of interaction with the radiation, it is expedient to use the most suitable geometrical parameter for the shape reconstruction. The most practical parameter is exactly the thickness, but in the case of weakly absorbing homogeneous materials, the error of the thickness calculation may be too large. For such cases it is more convenient to use the tilt angle of the surface, that may be calculated from the refraction angle. Although this method becomes highly inaccurate for the angles close to 90 degrees.

Figure 5 demonstrates the results of the shape reconstruction for the half-cylinder, those are based on the calculations of thickness and the tilt angles. The calculations were performed with zero distance from object to analyzer and with no inhomogeneities.

The calculations show, that the most accurate way to reconstruct the

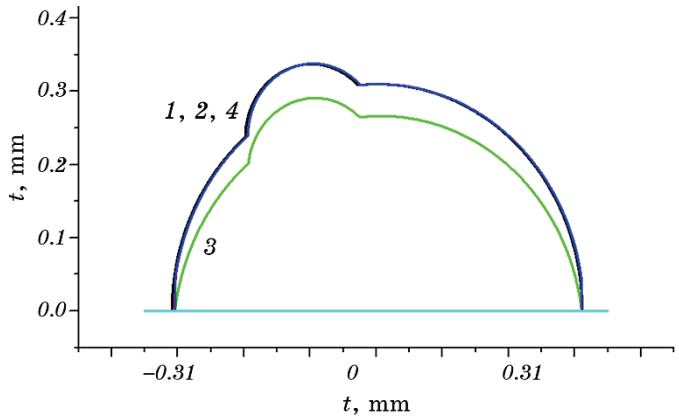

Fig. 5. The original shape (*1*) and the shape, reconstructed using only thickness (*2*), only tilt angle (*3*) and both the thickness and the tilt angle (*4*).

shape of such half-cylinder is to use both the thickness and the tilt angle at the same time, and thus by considering both absorption and refraction.

4. CONCLUSIONS

The work demonstrates the features of the ABI for non-crystalline objects, related with the impact on the imaging of the inhomogeneities of various scale both in the object and the monochromator and analyzer crystals. As it was shown, the scattering pattern substantially depends on the dynamical scattering effects in all the elements of the triple-axis imaging scheme.

Such instrumental factors as the scales and distances between the elements of optical scheme also have great influence, and thus are necessary to take into account.

The usage of the suggested theoretical approach, which strictly takes into account the radiation scattering in both the monochromator and the analyzer crystals, as well as in the object, allows resolving the inverse scattering problem, and, as the result, determining the geometrical properties of the non-crystalline sample. The results of the computations for the model object confirm such possibility and demonstrate important features of the shape reconstruction process.

This work was financially supported by N.A.S. of Ukraine, Project No. 5Φ.

REFERENCES

1. S. W. Wilkins, Ya. I. Nesterets, T. E. Gureyev, S. C. Mayo, A. Pogany, and A. W. Stevenson, *Phil. Trans. R. Soc. A*, **372**: 20130021 (2014).
2. A. Olivo and E. Castelli, *La Rivista del Nuovo Cimento*, Iss. 9: 467 (2014).
3. M. Endrizzi, *Nucl. Instrum. Methods A*, **878**: 88 (2018).
4. P. Suortti, J. Keyriläinen, and W. Thomlinson, *J. Phys. D: Appl. Phys.*, **46**, No. 49: 494002 (2013).
5. D. Chapman, W. Thomlinson, R. E. Johnston, D. Washburn, E. Pisano, N. Gmür, Z. Zhong, R. Menk, F. Arfelli, and D. Sayers, *Phys. Med. Biol.*, **42**, No. 11: 2015 (1997).
6. F. A. Dilmanian, Z. Zhong, B. Ren, X. Y. Wu, D. Chapman, I. Orion, and W. Thomlinson, *Phys. Med. Biol.*, **45**, No. 4: 933 (2000).
7. Y. I. Nesterets, P. Coan, T. E. Gureyev, A. Bravin, P. Cloetens, and S. W. Wilkins, *Acta Crystallogr. Sect. A*, **62**: 296 (2006).
8. H. Suhonen, M. Fernández, A. Bravin, J. Keyriläinen, and P. Suortti, *J. Synchrotron Radiat.*, **14**: 512 (2007).
9. M. J. Kitchen, K. M. Pavlov, K. K. W. Siu, R. H. Menk, G. Tromba, and R. A. Lewis, *Phys. Med. Biol.*, **52**, No. 14: 4171 (2007).
10. O. Oltulu, Z. Zhong, M. Hasnah, M. N. Wernick, and D. Chapman, *J. Phys. D:*

Appl. Phys., **36**, No. 17: 2152 (2003).
11. E. Pagot, P. Cloetens, S. Fiedler, A. Bravin, P. Coan, J. Baruchel, J. Härtwig, and W. Thomlinson, *Appl. Phys. Lett.*, **82**: 3421 (2003).
12. M. Wernick, O. Wirjadi, D. Chapman, Z. Zhong, N. P. Galatsanos, Y. Yang, J. G. Brankov, O. Oltulu, M. A. Anastasio, and C. Muehleman, *Phys. Med. Biol.*, **48**, No. 23: 3875 (2003).
13. Ya. I. Nesterets, T. E. Gureyev, D. Paganin, K. M. Pavlov, and S. W. Wilkins, *J. Phys. D: Appl. Phys.*, **37**, No. 8: 1262 (2004).
14. Ya. I. Nesterets, T. E. Gureyev, K. M. Pavlov, D. M. Paganin, and S. W. Wilkins, *Opt. Commun.*, **259**: 19 (2006).
15. B. V. Sheludchenko, V. B. Molodkin, S. V. Lizunova, S. J. Olikhovskii, Ye. M. Kyslovskyi, O. Yu. Gaevskyi, V. V. Lizunov, A. I. Nizkova, T. P. Vladimirova, V. V. Molodkin, K. V. Fuzyk, A. V. Goshkoderya, A. O. Bilotska, G. O. Velikhovskyi, A. A. Muzychenko, and R. V. Lekhnyak, *Metallofiz. Noveishie Tekhnol.*, **36**, No. 4: 559 (2014) (in Russian).
16. V. B. Molodkin, G. O. Velikhovskii, S. V. Lizunova, V. V. Lizunov, B. V. Sheludchenko, E. M. Kislovskii, Ya. V. Vasilik, O. S. Skakunova, S. V. Dmitriev, K. V. Fuzik, and R. V. Lekhnyak, *Materialwissenschaft und Werkstofftechnik*, **47**, Iss. 2–3: 246 (2016).
17. V. B. Molodkin, G. O. Velikhovskyi, S. V. Lizunova, and V. V. Lizunov, *Opt. Commun.*, **439**: 1 (2019).
18. M. A. Krivoglaz, *X-Ray and Neutron Diffraction in Nonideal Crystals* (Berlin: Springer: 1996).
19. G. Khelashvili, J. G. Brankov, D. Chapman, M. A. Anastasio, Y. Yang, Z. Zhong, and M. N. Wernick, *Phys. Med. Biol.*, **51**: 221 (2006).
20. S. V. Lizunova, V. B. Molodkin, B. V. Sheludchenko, and V. V. Lizunov, *Metallofiz. Noveishie Tekhnol.*, **35**, No. 11: 1585 (2013) (in Russian).
21. P. Coan, E. Pagot, S. Fiedler, P. Cloetens, J. Baruchel, and A. Bravin, *J. Synchrotron Radiation*, **12**: 241 (2005).